Selective Binding to Polynucleotides of the Hybrid Intercalating Groove Binder Bis(pyrrolecarboxamide)–Oxazolopyridocarbazole: A Molecular Modeling Study†

Hélène Goulaouic, Sandrine Carteau, Frédéric Subra, Jean François Mouscadet, and Christian Auclair*

Laboratoire de Pharmacologie Molèculaire, CNRS URA 147, INSERM U 140, Institut Gustave Roussy 94801, Villejuif, France

Jian-sheng Sun

Laboratoire de Biophysique, Museum National d'Histoire Naturelle, CNRS UA 481, INSERM U 201, 43 rue Cuvier, 75005 Paris, France

Received August 31, 1993; Revised Manuscript Received October 26, 1993®

ABSTRACT: In order to further characterize the binding of the hybrid molecule NetOPC [bis(pyrrolecarboxamide)–oxazolopyridocarbazole conjugate] to double-stranded DNA, we have performed a molecular modeling study to investigate the binding modes of the complexes possibly formed between NetOPC and synthetic polynucleotides poly $[(dA\text{-}dT)]_2$, poly [(dA)·(dT)], and poly $[d(G\text{-}C)]_2$ and interpreted the results in the light of the experimentally determined binding parameters. In agreement with experimental data, the modeling study suggests that whatever was the binding mode of the complex formed, the complexation energy is markedly lower (thus favorable) for AT-containing polynucleotides than for poly $d[(G\text{-}C)]_2$. With both poly [d(A)·d(T)] and poly $[d(A\text{-}T)]_2$, the most energetically favored complex has netropsin and OPC moieties bound simultaneously in the minor groove of DNA. The second favored complex exhibits the bimodal binding, i.e., intercalation of OPC and minor groove binding of the netropsin moiety. For both types of complex, the energy of complex formation is slightly lower with poly [d(A)·d(T)]. The binding site sizes of the modeled complexes are about seven and four base pairs to the full groove and bimodal binding, respectively.

In an attempt to obtain compounds susceptible to selectively alter genomic functions involving the recognition of AT-containing sequences (Dervan, 1982), we have previously synthesized (Subra et al., 1991; Mrani et al., 1991) a netropsin-like conjugate (Figure 1) in which the guanidine moiety of the netropsin molecule has been replaced by a tetramethylene chain linked to the intercalating chromophore oxazolopyridocarbazole (OPC) (Auclair et al., 1988). This molecule was further found to strongly inhibit the replicative cycle of Moloney Leukemia Virus (M.MuLV) likely through the interaction with the AT-rich sequences 5′-CTTTCATT of the LTR ends of the virus (Subra et al., 1993). In terms of DNA binding, the major interest expected from the presence of the OPC chromophore is the stabilization of the drug–DNA complex at the level of the recognized DNA sequence. According to this point of view, the ideal mode of interaction between the hybrid molecule and the double-strand DNA is supposed to consist of the intercalating binding of the OPC chromophore between DNA base pairs and the external binding of the netropsin moiety in the minor groove. In terms of thermodynamic parameters, this type of interaction should benefit from a large entropic contribution (14 cal mol^{-1} deg^{-1}) coming from the intercalation of the OPC chromophore (Schwaller, 1989) in the addition of the enthalpic contribution (−11 kcal mol^{-1}) coming from the external binding of netropsin moiety. This should lead to the occurrence of a high negative free-energy change upon DNA binding and, consequently, to a high association constant (K_{app}) value. Previous studies (Auclair et al., 1990; Subra et al., 1991) have shown that NetOPC was able to bind to poly $d[A\text{-}T)]_2$ according to high (K_{app} = 6 × 10^8 M^{-1}) and lower (K_{app} = 7.1 × 10^6 M^{-1}) affinity binding modes. In contrast, the binding to poly $d[(G\text{-}C)]_2$ occurs according to a single binding mode of low affinity (K_{app} = 1.7 × 10^6 M^{-1}). In agreement with thermodynamic considerations as stated above, NetOPC in the high-affinity binding mode showed higher association constant value to poly $d[(A\text{-}T)]_2$ as compared to netropsin. However, the different binding parameters investigated, including the apparent binding size and the number of charges involved in the binding (8 bp and two positive charges for the high-affinity binding mode, 3 bp and one positive charge for the low-affinity binding mode), as well as viscometric and energy-transfer data have not allowed us to draw conclusions on the nature of the complex of higher affinity or on the simultaneous binding through both intercalation of OPC chromophore and external binding of netropsin moiety in the minor groove of AT-rich sequences. In order to obtain additional information on the binding modes of NetOPC to DNA, we have undertaken a molecular modeling study of the complexes possibly formed between NetOPC and polynucleotides, in conjunction with a physicochemical study.

MATERIALS AND METHODS

Synthesis of OPC, Pentyl-OPC, and Netropsin–OPC conjugate. Oxazolopyridocarbazole (OPC) and pentyl-OPC were synthesized as previously described (Auclair & Paoletti, 1981; Auclair et al., 1984, 1988). The netropsin–OPC conjugate (NetOPC) was synthesized according to Mrani et al. (1992) and provided by Professor J. L. Imbach (Montpellier, France).

DNAs and Polynucleotides. DNA from *Micrococcus lysodeikticus* and *Clostridium perfringens*, poly $[d(A\text{-}T)]_2$,

† This work was supported by the ANRS Antiviral Research Program and ARC Grant 2035.

* To whom correspondence should be addressed.

® Abstract published in *Advance ACS Abstracts,* January 15, 1994.

0006-2960/94/0433-1412$04.50/0

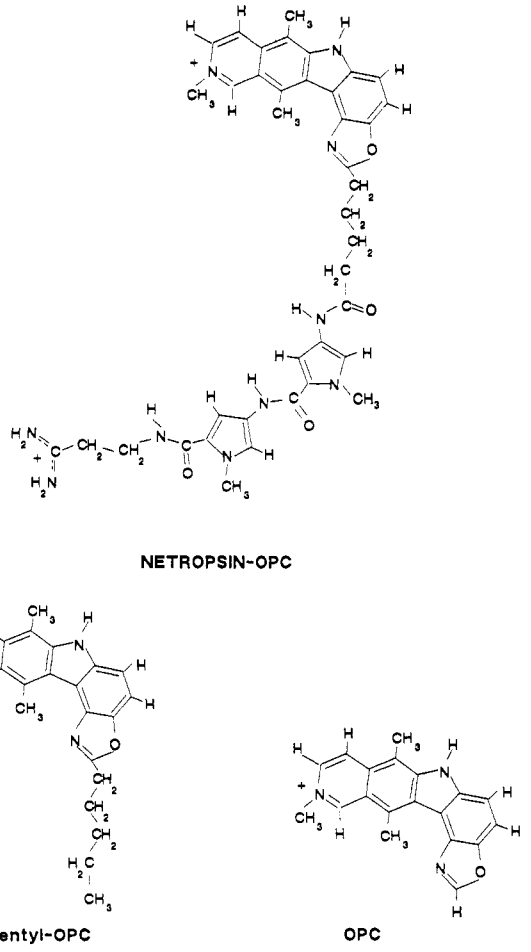

FIGURE 1: Structure of OPC, pentyl-OPC, and the hybrid molecule NetOPC.

poly [d(A)·d(T)], and poly d[(G-C)]$_2$ were obtained from Boehringer, Germany, and used after sonication (7 × 1 min) in a ice bath.

Association Constants to DNA. The association constant values of NetOPC to poly [d(A)·d(T)] were measured using the fluorescence increase (Le Pecq & Paoletti, 1967) of the OPC chromophore upon binding to a double-stranded polynucleotide as previously described (Subra et al., 1991).

Energy Transfer. The occurrence of an energy transfer from nucleic acids to the bound drug was determined according to Weil and Calvin (1963). The relative quantum yield ratio of the bound drug upon excitation in the UV region vs excitation in the visible region was determined by using the following equation:

$$\frac{Q_l}{Q_{vis}} = \left(\frac{I_{UV}}{I_{vis}}\frac{E_{vis}}{E_{UV}}\text{ bound}\right)\left(\frac{I_{vis}}{I_{UV}}\frac{E_{UV}}{E_{vis}}\text{ free}\right)$$

where I and E are respectively the fluorescence intensity and the molar extinction coefficient for exc, vis = 315 nm and exc, UV = 260 nm.

Viscometric Experiments. Viscometric measurements were performed at 25 °C in a semi-microdilution capillary viscometer linked to a IBM XT computer. The capacity of tested compounds to increase the length of sonicated DNAs and polynucleotides was measured using standard operating conditions (Saucier et al., 1971). In the conditions used (0.01 M acetate buffer, pH 5.5, 0.1 M NaCl), the slope value describing the length increase of sonicated calf thymus DNA upon ligand binding was found to be 2.15 ± 0.06 for ethidium bromide taken as the reference intercalating agent.

Table 1: Binding Parameters of NetOPC to Synthetic Polynucleotides[a]

	poly[(dA)·(dT)]		poly[d(A-T)]		poly[d(G-C)]
	S_1	S_2	S_1	S_2	S_1
K_{app}[b]	8.6×10^8	2.4×10^6	6.0×10^8	7.2×10^6	1.72×10^6
slope[c]	−1.68	−0.89	−1.62	−0.92	−0.64
n[d]	9.8	2.1	8.1	2.9	2.2
slope[e]	0.80		0.85		1.54
E_t[f]	2.25		2.30		2.82

[a] S_1 and S_2 refer to the different binding sites. [b] Association constant values calculated from the best fit to data points of the binding curves represented as rectangular hyperbola. [c] Slope of the straight line obtained from the linear regression of the equation describing the variation of the K_{app} as a function of the ionic strength such as $\log K_{app}/\log [Na^+] = -Z\xi$ (Record, 1976). [d] Apparent size of binding site as estimated from the best fit to data points of the binding curves. [e] Slope of the straight line obtained from the linear regression of the equation describing the variation of the viscosity of DNA as a function of NetOPC bound such as $\log n/n_o = \log(1 + 2r)$ (Saucier et al., 1971). [f] Excitation energy-transfer efficiency (E_t) from DNA bases to bound NetOPC. In the operating conditions used, the E_t value for intercalated OPC chromophore either in AT- or GC-containing polynucleotides is close to 6.

Circular Dichroism. CD spectra were recorded on a Roussel-Jouan dichrograph Mark IV. Samples were placed in a quartz cell (3 mL, 1-cm path length) thermostated at 25 °C. In typical experiments, DNA concentrations were 70 μM. Data were stored in a Minc 11/23 computer and corrected for the dichroism of the buffer.

Molecular Modeling. Conformational enthalpy minimization has been performed with the *JUMNA* (Junction Minimization of Nucleic Acids) program package (Lavery, 1988) which use helicoidal coordinates particularly suitable for nucleic acids. Recent developments of the *JUMNA* program package allow us to include any number of nonbonded ligands into the calculations with the help of the *Nchem* (Nucleotide Chemistry) program. The oxazolopyridocarbazole derivative (OPC), netropsin, and the hybrid NetOPC conjugate molecules have been built using the Insight II graphical program developed by Biosym Technology Inc. and then charged and analyzed by *Nchem* to prepare a data file containing geometrical parameters, atomic charges, and flexibility information for use in the *JUMNA* program (see supplementary material). Charges of ligands were calculated with a Huckel–Del Re procedure, which was parametrized on the basis of quantum calculations (Lavery et al., 1984). Neither water nor counter-ions were explicitly included in this calculation. Their effects were simulated by using a sigmoidal distance-dependent dielectric function (Lavery et al., 1986) and by assigning a half-charge on the phosphate group.

The first step in the computing procedure consists of building up the DNA fragment, which consists of 13 base pairs in double helix, and positioning the various nucleotides by means of their helical coordinates relative to the global axis system. Helicoidal coordinates are derived from published data obtained by crystallography on the B-DNA double helix (Arnott et al., 1980). The rise parameter was doubled at the intercalation site, and the twist was subsequently reduced in order to create an intercalation site. The interactive docking of the ligand–DNA complex was achieved manually by using Insight II software to avoid steric clashes.

In early stages of minimization, the helicoidal variables and/or the sugar–phosphate backbone, as well as ligand variables, could be locked. Minimization was performed by successively decreasing the number of constraints. Finally, all variables were free to evolve until the energy convergence

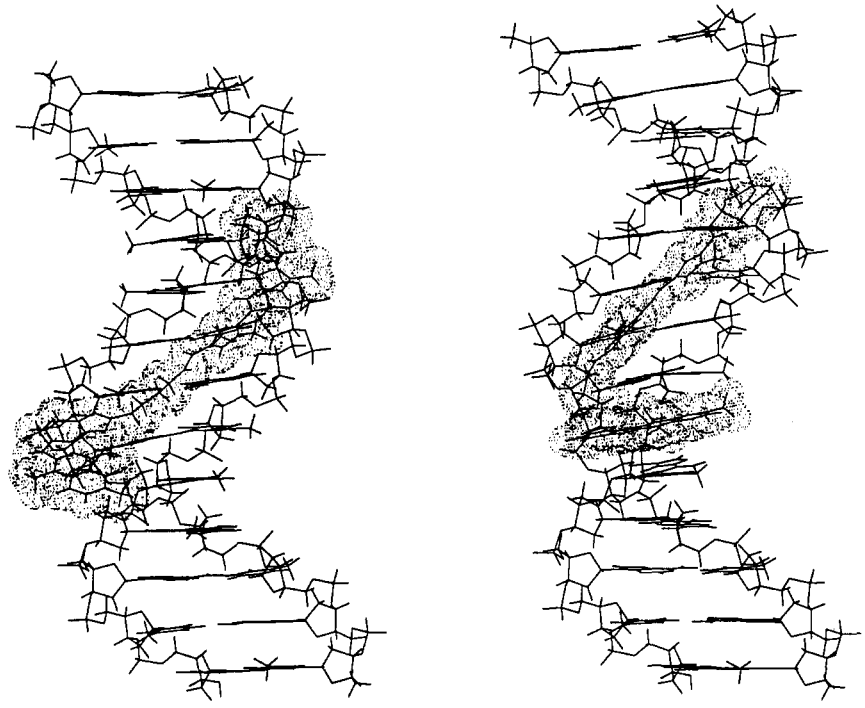

FIGURE 2: Molecular picture of the best energy-minimized NetOPC poly[d(A-T)]$_2$ complexes. The dot surface delimits the van der Waals radii of the NetOPC molecule. (Left panel) NetOPC–DNA complex in a simultaneous groove binding of OPC and netropsin moieties. (Right panel). NetOPC–DNA complex in a bimodal binding, i.e., the intercalation of OPC and the minor groove binding of netropsin.

criterion was reached. In a effort to reduce the end effect, the last four base pairs of each end were constrained to mono- or dinucleotide symmetry for poly d[d(A)·(dT)] or poly [d(A-T)]$_2$ and poly [d(G-C)]$_2$, respectively. To overcome the local energy minima, several starting conformations have been used with different ligand docking, i.e., the OPC moiety was put in various positions with respect to netropsin and double-stranded DNA. The obtained optimal structure was subsequently subjected to stretching compression as well as under- and overtwisting deformation by imposing a quadratic constraint on the total rise or twist on the oligomer. This technique ensures the stability of the local minimal energy conformation over an extended range of helicoidal parameters and provides a convenient way to escape the local minima problem (Poncin et al., 1992a,b). Only the best energy complexes were presented and analyzed by the *CURVE* (Lavery & Sklenar, 1989) program, which determine the helicoidal parameters of all the bases with respect to a global axis derived by a least-squares fit. These computations were performed on a Silicone Graphics 4D/420GTXB workstation, and the molecules were visualized with the help of Insight II fully interfaced with JUMNA.

RESULTS AND DISCUSSION

Binding Parameters of NetOPC to Synthetic Polynucleotides Poly[(dA-dT)]$_2$, Poly[d(A)·d(T)], and Poly[(dG-dC)]$_2$. In a previous work, we determined the association constant values of NetOPC for synthetic polynucleotides poly [(dA-dT)]$_2$ and poly [(dG-dC)]$_2$ as well as two physicochemical measurements suggestive to intercalation (length increase of sonicated DNA and excitation energy transfer) using natural DNAs of various base pairs composition. In order to interpret data provided by molecular modeling in which modeled DNA were poly [(dA·dT)]$_2$ and poly [d(G-C)]$_2$, we have first of all further determined the K_{app} values of NetOPC to poly(dA)·poly(dT) and intercalation parameters using as DNA the three polynucleotides modelized. Data obtained are summarized in Table 1. As previously described (Subra et al., 1991), the binding of NetOPC to poly[(dA-dT)]$_2$ occurs at two different sites. The first one of high affinity ($K_{app} = 6 \times 10^8$ M^{-1}) displays an apparent size of about 8 bp, and the second one of lower affinity (1.72×10^6 M^{-1}) displays an apparent size of about 3 bp. The number of charges involved in the binding as estimated according to Record et al. (1976) appears to be close to two for the high-affinity site and close to one for the lower affinity site. Finally, the parameters related to intercalation and provided by viscometry (Saucier et al., 1971) of sonicated poly[(dA-dT)]$_2$ and energy transfer (Rheinart et al., 1982) (see Materials and Methods) suggest that either the OPC chromophore is partly intercalated in both binding sites or that OPC is intercalated in only one of the two binding sites. Similar results are observed using poly-[(dA)·(dT)] except that a higher K_{app} value was observed for the high-affinity site (S1) and a lower value for the weak-affinity site (S2). In contrast, the binding of NetOPC to poly[d(G-C)]$_2$ involves a single type of binding site. The K_{app} value is close to 2×10^6 M^{-1}, and one positive charge is involved in the binding. The apparent binding site size of 2.2 is close to the values obtained with typical intercalating agents. Thus, the viscometric and energy-transfer data were well consistent with the intercalation of the OPC chromophore.

Molecular Modeling. The molecular modeling study of the complexes between NetOPC and double-standard polynucleotides was carried out with the fragments of 13 bp in length. They were chosen to simulate the complexation of NetOPC with poly[d(A)·d(T)], poly[(dA-dT)]$_2$, and poly-[(dG-dC)]$_2$, respectively. Figure 2 shows two molecular pictures of the best energy-minimized NetOPC–DNA complexes possibly formed in which one was in simultaneous groove binding of both OPC and netropsin moieties (Figure 2, left) and another was in the bimodal binding (Figure 2, right). It can be seen that there were not major conformational alterations on the double-stranded DNA in both models. The actual binding sites were about 7 and 4 bp, corresponding to

Table 2: Energy Decomposition of the NetOPC–Polynucleotide Complexes[a]

DNA	binding mode		ΔE_{DNA}	ΔE_{LIG}	LJ	$E_{LIG-DNA}$ elec	total	E_C
	OPC	netropsin						
p(dA)·p(dT)	I	g	+30.1	+10.4	−84.0	−77.4	−161.4	−120.9
p(dA)·p(dT)	g	g	+6.7	+14.1	−76.4	−97.4	−173.8	−153.0
p(dA-dT)·p(dA-dT)	I	g	+29.6	+13.5	−80.7	−80.8	−161.5	−118.4
p(dA-dT)·p(dA-dT)	g	g	+11.7	+12.6	−75.2	−97.2	−172.4	−148.1
p(dG-dC)·p(dG-dC)	I	g	+32.0	+13.4	−73.2	−70.2	−143.4	−98.0
p(dG-dC)·p(dG-dC)	g	g	+14.7	+6.2	−63.4	−69.3	−132.7	−111.8
p(dG-dC)·p(dG-dC)	I	G	+24.7	+17.5	−59.3	−87.2	−146.5	−104.3
p(dG-dC)·p(dG-dC)	G	G	+13.1	+16.1	−46.9	−100.0	−146.9	−117.7

[a] The letters I, g, and G show that the indicated moiety is in an intercalation, in a minor groove, or in a major groove binding mode, respectively. The ligand–DNA interaction ($E_{LIG-DNA}$) is decomposed in Lennard–Jones (LJ) and electrostatic (elec) terms. ΔE_{DNA} and ΔE_{LIG} are the deformation energy of the DNA and the ligand, respectively. The complexation energy (E_C) is the sum of the ligand–DNA interaction and the deformation energies. Energy unit is kcal mol^{-1}.

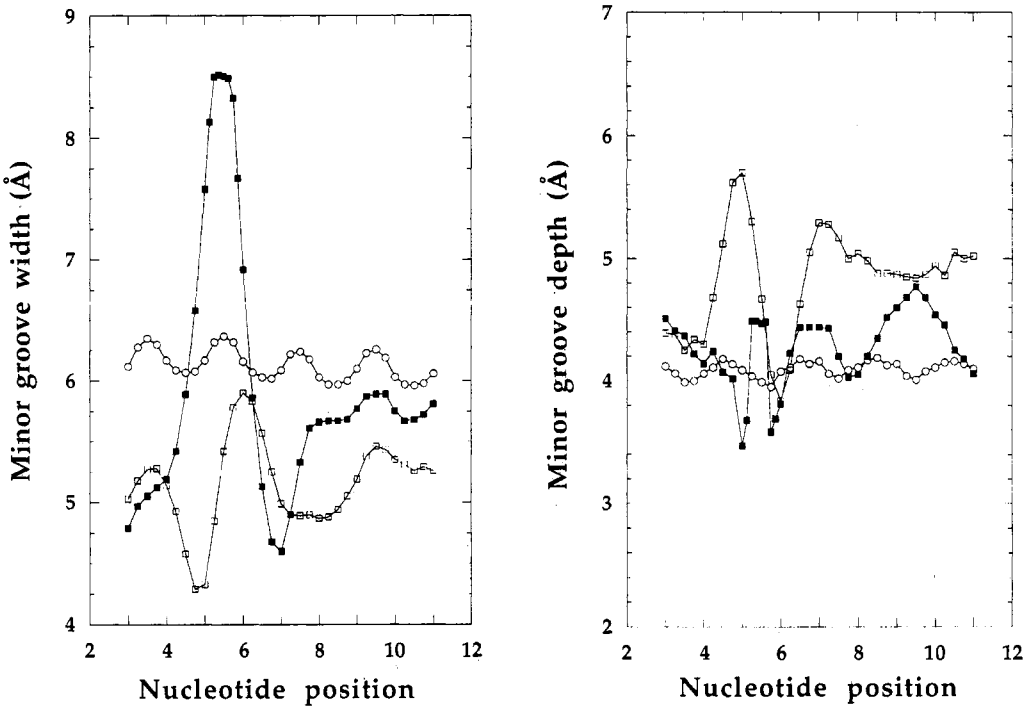

FIGURE 3: Variation of the minor groove width and depth of the best energy-minimized NetOPC poly [d(A-T)]$_2$ complexes. The open circles, open squares, and filled squares indicate the native DNA oligomer, the NetOPC–oligomer complex according to full groove or the NetOPC-oligomer complex according bimodel binding, respectively.

the full groove binding (strong site) and the bimodal binding (weak site), respectively. The conformational energy of energy-minimized ligand–DNA complexes can be decomposed into the following terms: (1) ΔE_{DNA} and ΔE_{LIG}, which are deformation energy upon complexation of DNA or ligand molecule, respectively; (2) $E_{LIg-DNA}$, which represent the ligand DNA interaction energy and is further split into Lennard–Jones (LJ) and electrostatic (Elec) components. E_{tot} is the sum of Lennard–Jones and electrostatic interactions; (3) E_C, which is the energy of complex formation represented by the sum of ΔE_{DNA}, ΔE_{LIG}, and $\Delta E_{LIG-DNA}$.

Table 2 summarizes the energy decomposition of the best energy-minimized ligand–DNA complexes. For all three sequences studied, the most favored complex had both netropsin and OPC moieties bound simultaneously in the minor groove of DNA. The second favored complex exhibited the bimodal binding, i.e., intercalation of OPC and minor groove binding, of the netropsin moiety. It can be seen that the difference on the complexation energy in favor of the former complex mainly from the low deformation energy upon complexation of DNA and secondly from the ligand–DNA interaction (especially for AT-rich sequences). It can be explained by the fact that the intercalative binding of OPC moiety requires a relative high cost in terms of DNA deformation energy due to the obligatory destacking of two consecutive base pairs and resulting in some local distorsions of helical and backbone conformation at the intercalation site (Figure 3). However, it should be noted that when OPC chromophore is bound in the groove of DNA, the DNA deformation and the ligand–DNA interaction might be under- or overestimated, respectively. This misevaluation could be ascribed to the computational approximation, namely, neither water molecules nor counter-ions were explicitly taken into account in current calculations. Consequently, the complexation energy of the full groove binding of NetOPC might be overestimated as compared to the bimodal binding and the extent of overestimation depends also on the DNA sequence. Nevertheless, given the large difference of the complexation energy (about 30 kcal mol^{-1}) bewtween two binding modes in AT-rich sequences, it was unlikely that the quantitative correction of hydration effect would reverse the qualitative tendancy in favor of the full groove binding of NetOPC in AT-rich sequence. In addition, data provided by the binding experiments in solution supported this proposal. In both AT-

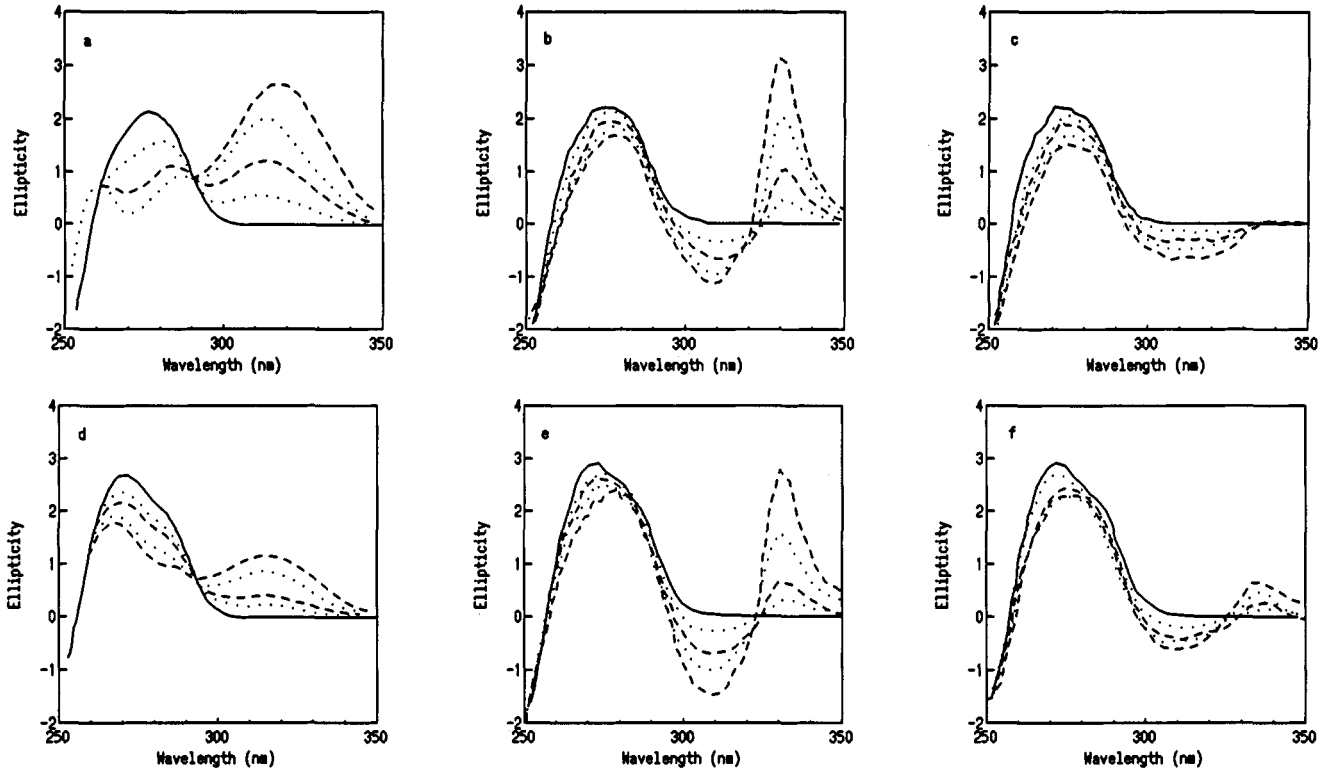

FIGURE 4: Circular dichroism spectra of DNA from *Clostridium* (panels a–c) and *Micrococcus* (panels d–f) in the presence of increasing concentrations of netropsin (a, d), OPC (b, e), and pentyl-OPC (c, f). Spectra were recorded at 25 °C. In all experiments, the assay medium was composed of cacodylate buffer 10 mM (pH 7.0), 100 mM NaCl, and 70 μM DNA and increasing ligands to nucleotide ratio (r') as follows: a and d, $r' = 0$, 0.01, 0.03, 0.06, and 0.1; b, c, e, and f, $r' = 0$, 0.5, 0.1, 0.15, and 0.2.

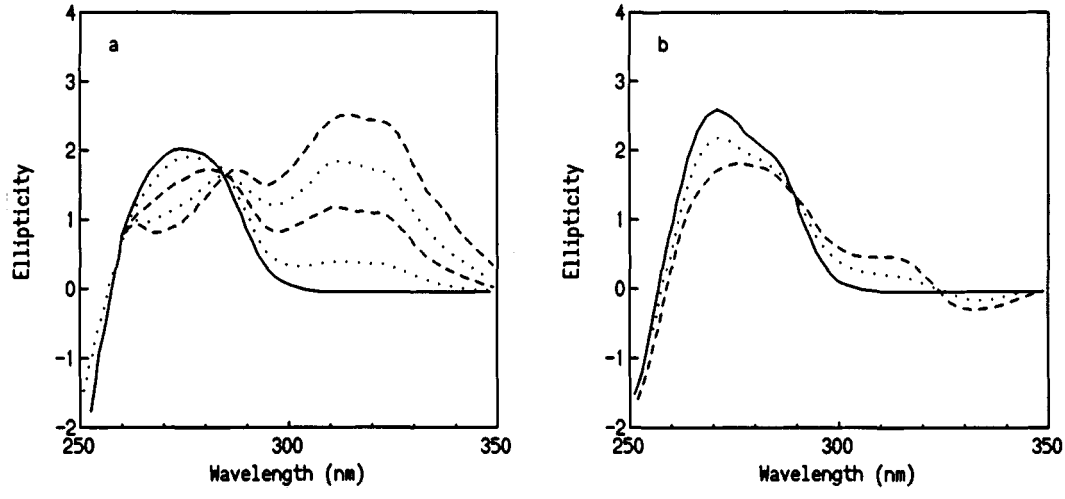

FIGURE 5: Circular dichroism spectra of DNA from *Clostridium* (panel a) and *Micrococcus* (panel b) in the presence of increasing concentrations of NetOPC. Compositions of the mixtures were as in the legend of Figure 3. $r' = 0$, 0.01, 0.03, 0.06, and 0.1.

containing polynucleotides, the size of the strong site provided by the Scatchard plot (8–9 base pairs) was slightly longer than but still close to that of the actual binding site of the full groove binding complex (seven base pairs). This slight discrepancy could be explained by the presence of terminal charges located at both ends of NetOPC conjugate, thus preventing the adjacent binding of another NetOPC molecule. Secondly, the strong site involved two positive charges in the binding whereas the weak site involves only one, which is in agreement with the marked difference (20 kcal mol^{-1}) existing between the electrostatic forces characterizing the full groove binding and the bimodal binding. Furthermore, it was remarked that there are two accessible charged groups in the full groove binding instead of only one (amidinium) in the bimodal binding mode. This was also in agreement with the effect of ionic strength on two binding modes. Therefore, the actual binding mode of NetOPC to AT-containing sequences was consistent with the occurrence of two modes: (i) a full groove binding mode (strong site) in which both netropsin and OPC lie in the minor groove and (ii) a bimodal mode (weak site) in which OPC is intercalated between base pairs whereas the netropsin moiety lies in the minor groove. However, it turns out that the complexation energy of such complexes were significantly higher (thus less favorable) than those of the NetOPCD with AT-rich sequences. These differences were more pronounced in the full groove binding mode, suggesting that the former binding mode might comparatively be less energetically favorable than the later mode. Finally, the role of the linker between OPC and netropsin moieties was also investigated by modeling. It

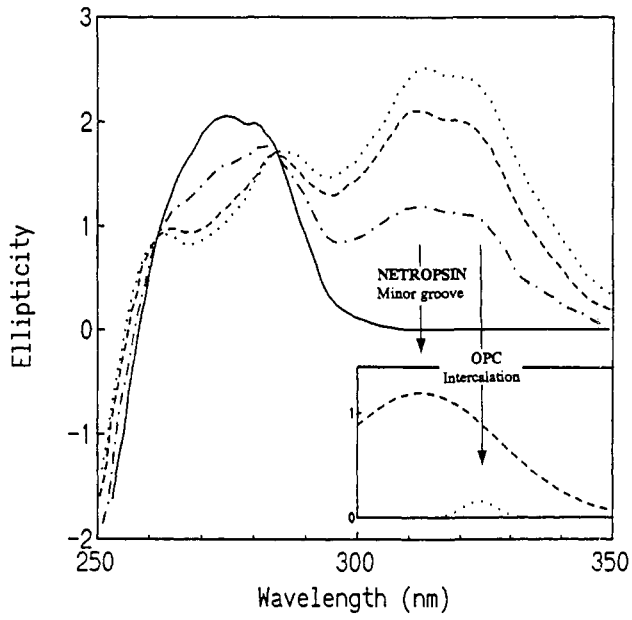

FIGURE 6: Circular dichroism spectra of DNA from *Clostridium* in the presence of increasing concentrations of NetOPC. Compositions of the mixtures were as in the legend of Figure 3. $r' = 0, 0.03, 0.06$, and 0.1. (Insert) Deconvolution of the CD spectrum obtained for $r' = 0.03$. The fitted spectra were obtained from the deconvolution of the CD spectrum in two Gaussians. The best fit to data points yields a correlation coefficient $r = 0.99$.

appears that the shortening of the tetramethylene linker to the trimethylene one favored the bimodal binding mode (data not shown). As matter of fact, this is due to a phasing effect, i.e., a trimethylene linker did not allow NetOPC to adopt a suitable concave shape in order to bind in the groove. It has been proven that another intercalator groove binder conjugate (Distel) using a trimethylene linker exhibited only bimodal binding with DNA (Bourdouxhe et al., 1992).

The structural conformation of different NetOPC–DNA complexes remains close to B-like DNA. As usual, the rise was increased to about 7 Å, and subsequently, the twist was reduced to about 18° at the intercalation site, T5pA6. We found, in agreement with numerous works, that the TpA step is more favorable than the ApT step for intercalation (data not shown). Figure 3 shows the variation of the minor groove width and depth of oligomer with alternating AT sequence upon the complexation of netOPC. The minor groove width and depth of native DNA are about 6 and 4 Å, respectively. This relatively wide groove width is consistent with recently published work, which shows that the narrow minor groove found in the AT-rich tract of Dickerson's dodecamer and other related cristal structures is likely a property of this peculiar sequences (Boutonnet et al., 1992). It is worth noticing that (i) the bimodal binding induced a marked local increase of minor groove width, which is associated with high rise and low twist changes at the intercalation site, while the minor groove depth remains essentially the same as the native DNA and (ii) conversely, both minor groove width and depth exhibited correlated changes for full groove binding mode, especially located near the OPC moiety end.

Circular Dichroism Study. Information related to the nature of the actual NetOPC–DNA complexes coexisting in solution can be provided by circular dichroism experiments. We have first of all recorded the induced CD spectra obained with mixtures containing natural DNA purified either from *Clostridium perfringens* (containing 68% AT base pairs) or from *Micrococcus lysodeikticus* (containing 72% GC base pairs) and containing the intercalating chromophore OPC, the outside binder pentyl-OPC (Le Ber et al., 1989), and netropsin. The aim of this set of experiments is to characterize, respectively, the induced spectra of OPC intercalated between base pairs; OPC bound according to external mode; and netropsin bound in the minor groove. Figure 4a–c shows the CD spectra of DNA from *Clostridium* recorded in the presence of increasing concentrations of each tested compound. As previously reported, it can be seen that the binding of netropsin (panel a) results in the appearance of an induced signal in the absorption region of the complex. The binding of OPC (panel b) to the polynucleotide results in the appearance of a strong induced assymetric signal in the range of the absorption of the drug–DNA complex. In contrast, the binding of the external binder derivative pentyl-OPC (panel c) results in a slight change of the polynucleotide CD spectra. In the presence of DNA from *Micrococcus* (Figure 4d–f), similar results were obtained except that netropsin (panel d) induces a lower alteration of the DNA spectra resulting from the lower binding efficiency of this compound to GC sequences whereas both OPC (panel e) and pentyl-OPC (panel f) binding results in the appearance of a more symetric signal. The shape of the CD spectra of drug–DNA complexes can be interpreted according to at least two different assumptions. First, it has been suggested that the sign of CD signal depends on the angular orientation of the intercalator relative to the base pair dyad axis (Lyng et al., 1987). Negative signal was then attributed to intercalated chromophore perpendicular to the dyad axis whereas positive signal reflects an orientation parallel to the dyad axis. CD spectra as in Figure 4b could be therefore consistent with the superposition of two spectra of the opposite sign that are shifted relative to each other and coming from at least two different intercalation geometries with a significant preference for the parallel orientation (positive spectra). The second possibility is that the symmetric component of the spectra could be attributed to an excitonic-like signal resulting from intermolecular ligand–ligand interactions (Monnot et al., 1992) whereas the positive signal could be attributed to intercalation only. Figure 5a,b shows the CD spectra of DNA from *Clostridium* and from *Micrococcus* recorded in the presence of increasing concentrations of NetOPC. In Figure 5a, it can be seen that the induced spectra resulting from the binding of NetOPC to AT-rich sequences clearly displays superimposed signals. From the spectra recorded in the presence of pentyl-OPC, it can be assumed that, in AT-rich sequences, the contribution to CD signal of OPC complexed to DNA according to external binding mode is negligible. The NetOPC-induced signals could be therefore attributed to netropsin (maximum 318 nm) and to OPC intercalated between bases pairs (maximum 330 nm). It should be noticed that molecular modeling shows that in the NetOPC–DNA bimodal complex, OPC is mainly parallel to the dyad axis. This single possible orientation should result in the occurrence of a positive CD signal only. Based on this consideration, the deconvolution of the two induces signals is therefore feasible in any case and shown in Figure 6. It can be seen that the main part of the signal comes from the complex between netropsin moiety and DNA. Regarding the data provided by the binding parameters and molecular modeling, these results suggest that, in solution and at the equilibrium, NetOPC actually binds to AT sequences according to both full groove and bimodal binding modes. Because of its higher K_{app}, the population of the NetOPC–DNA complexes is mainly constituted of the full groove complex. In *Micrococcus* DNA, the binding of NetOPC results in the appearance of a weak-

induced spectra which cannot be characterized either in term of netropsin binding or in term of intercalation of OPC. This can be attributed to the possible binding of NetOPC to major groove, which remains uncharacterized in terms of spectral properties. Similar results have been obtained with the synthetic polynucleotides poly d[(A-T)]$_2$ and poly d[(G-C)]$_2$ (data not shown).

SUPPLEMENTARY MATERIAL AVAILABLE

Partial atomic charges, coordinates of Net-OPC, controle files and parameters for *JUMNA, Nchem, and Curve* calculations (7 pages). Ordering information is given on any current masthead page.

REFERENCES

Arnott, S., Chandrasekharan, R., Birsdall, D. L., Leslie, A. G. W., & Tatliff, R. L. (1980) *Nature 283*, 743–745.

Auclair, C., & Paoletti, C. (1981) *J. Med. Chem. 24*, 289–295.

Auclair, C., Voisin, E., Banoun, H., Paoletti, C., Bernadou, J., & Meunier, B. (1984) *J. Med. Chem. 27*, 1161–1166.

Auclair, C., Schwaller, M. A., René, B., Banoun, H., Saucier, J. M., & Larsen, A. K. (1988) *Anti-Cancer Drug Des. 3*, 133–144.

Auclair, C., Subra, F., Mrani, D., Gosselin, G., Imbach, J. L., & Paoletti, C. (1990) in *Molecular Basis of Specificity in Nucleic Acid-Drug Interactions*, Pullman, B., Jortner, J., pp 247–260, Kluwer Academic Publishers, Dordrecht, The Netherlands.

Boutonnet, N., Hui, X. W., & Zakrzewska, K. (1993) *Biopolymers 33*, 479–490.

Dervan, P. B. (1986) *Science 232*, 464–471.

Lavery, R., & Sklenar, H. (1989) *J. Biomol. Struct. Dyn. 6*, 655–667.

Lavery, R., Zakrzewska, K., & Pulmann, B. (1984) *J. Comput. Chem. 5*, 363–373.

Lavery, R., Sklenar, H., Zakrzewska, K., & Pulmann, B. (1986) *J. Biomol. Struct. Dyn. 3*, 929–1014.

Lavery, R. (1988) in *Structure and Expression; Vol. 3, DNA Bending and Curvature*, Olson, W. K., Sarm, M. H. Sarma, R. H., & Sundaralingam, Eds.) pp 191–211, Adenine Press, New York.

Le Ber, P., Schwaller, M. A., & Auclair, C. (1989) *J. Mol. Recognit. 2*, 152–157.

Le Pecq, J. B., & Paoletti, C. (1967) *J. Mol. Biol. 27*, 87–106.

Lyng, R., Härd, T., & Norden, B. (1987) *Biopolymers 26*, 1327–1345.

Monnot, M., Mauffret, O., Lescot, E., & Fermandjian, S. (1992) *Eur. J. Biochem. 104*, 1035–1039.

Mrani, D., Gosselin, G., Auclair, C., Balzarini, J., De Clercq, E., Paoletti, C., & Imbach, J. L. (1991) *Eur. J. Med. Chem. 26*, 481–488.

Poncin, M., Hartmann, B., & Lavery, R. (1992a) *J. Mol. Biol 226*, 775–794.

Poncin, M., Piazzola, D., & Lavery, R. (1992b) *Biopolymers 32*, 1077–1103.

Record, M. T., Lohman, T. M., & de Haseth, P. (1976) *J. Mol. Biol. 107*, 145–158.

Reinhardt, C. G., Roques, B. P., & Le Pecq, J. B. (1982) *Biochem. Biophys. Res. Commun. 4*, 1376–385.

Saucier, J. M., Festy, B., & Le Pecq, J. B. (1971) *Biochimie 53*, 973–979.

Schwaller, M. A. (1989) *Thesis*, University Paris VI.

Subra, F., Carteau, S., Pager, J., Paoletti, J., Paoletti, C., Auclair, C., Mrani, D., Gosselin, G., & Imbach, J. L. (1991) *Biochemistry 30*, 1642–1650.

Subra, F., Mouscadet, J. F., Lavignon, M., Roy, C., & Auclair, C. (1993) *Biochem. Pharmacol. 45*, 93–99.

Weil, G., & Calvin, M. (1963) *Biopolymers 1*, 401–409.